

Biogeosciences, 13, 1129–1144, 2016

www.biogeosciences.net/13/1129/2016/

doi:10.5194/bg-13-1129-2016

© Author(s) 2016. CC Attribution 3.0 License.



Oxygen isotope fractionation during N₂O production by soil denitrification

Dominika Lewicka-Szczebak¹, Jens Dyckmans³, Jan Kaiser², Alina Marca², Jürgen Augustin⁴, and Reinhard Well¹¹Thünen Institute of Climate-Smart Agriculture, Federal Research Institute for Rural Areas, Forestry and Fisheries, Bundesallee 50, 38116 Braunschweig, Germany²Centre for Ocean and Atmospheric Sciences, School of Environmental Sciences, University of East Anglia, Norwich, NR4 7TJ, UK³Centre for Stable Isotope Research and Analysis, University of Göttingen, Büsingenweg 2, 37077 Göttingen, Germany⁴Leibniz Centre for Agricultural Landscape Research, Eberswalder Straße 84, 15374 Müncheberg, GermanyCorrespondence to: Dominika Lewicka-Szczebak (dominika.lewicka-szczebak@vti.bund.de)

Received: 15 September 2015 – Published in Biogeosciences Discuss.: 22 October 2015

Revised: 19 January 2016 – Accepted: 5 February 2016 – Published: 24 February 2016

Abstract. The isotopic composition of soil-derived N₂O can help differentiate between N₂O production pathways and estimate the fraction of N₂O reduced to N₂. Until now, δ¹⁸O of N₂O has been rarely used in the interpretation of N₂O isotopic signatures because of the rather complex oxygen isotope fractionations during N₂O production by denitrification. The latter process involves nitrate reduction mediated through the following three enzymes: nitrate reductase (NAR), nitrite reductase (NIR) and nitric oxide reductase (NOR). Each step removes one oxygen atom as water (H₂O), which gives rise to a branching isotope effect. Moreover, denitrification intermediates may partially or fully exchange oxygen isotopes with ambient water, which is associated with an exchange isotope effect. The main objective of this study was to decipher the mechanism of oxygen isotope fractionation during N₂O production by soil denitrification and, in particular, to investigate the relationship between the extent of oxygen isotope exchange with soil water and the δ¹⁸O values of the produced N₂O.

In our soil incubation experiments Δ¹⁷O isotope tracing was applied for the first time to simultaneously determine the extent of oxygen isotope exchange and any associated oxygen isotope effect. We found that N₂O formation in static anoxic incubation experiments was typically associated with oxygen isotope exchange close to 100 % and a stable difference between the ¹⁸O/¹⁶O ratio of soil water and the N₂O product of δ¹⁸O(N₂O/H₂O) = (17.5 ± 1.2) ‰. However, flow-through experiments gave lower oxygen isotope ex-

change down to 56 % and a higher δ¹⁸O(N₂O/H₂O) of up to 37 ‰. The extent of isotope exchange and δ¹⁸O(N₂O/H₂O) showed a significant correlation ($R^2 = 0.70$, $p < 0.00001$). We hypothesize that this observation was due to the contribution of N₂O from another production process, most probably fungal denitrification.

An oxygen isotope fractionation model was used to test various scenarios with different magnitudes of branching isotope effects at different steps in the reduction process. The results suggest that during denitrification, isotope exchange occurs prior to isotope branching and that this exchange is mostly associated with the enzymatic nitrite reduction mediated by NIR. For bacterial denitrification, the branching isotope effect can be surprisingly low, about (0.0 ± 0.9) ‰, in contrast to fungal denitrification where higher values of up to 30 ‰ have been reported previously. This suggests that δ¹⁸O might be used as a tracer for differentiation between bacterial and fungal denitrification, due to their different magnitudes of branching isotope effects.

1 Introduction

Our ability to mitigate soil N₂O emissions is limited due to poor understanding of the complex interplay between N₂O production pathways in soil environments. In order to develop effective fertilizing strategies and reduce the loss of nitrogen through microbial consumption as well as related

adverse environmental impacts (IPCC, 2013; Ravishankara et al., 2009), it is very important to fill the existing knowledge gaps. Isotopocule analyses of N₂O, including $\delta^{18}\text{O}$, average $\delta^{15}\text{N}$ ($\delta^{15}\text{N}^{\text{av}}$) and ^{15}N site preference within the linear N₂O molecule ($\delta^{15}\text{N}^{\text{sp}}$) have been used for several years to help differentiate between N₂O production pathways (Opdyke et al., 2009; Perez et al., 2006; Sutka et al., 2006; Toyoda et al., 2005; Well et al., 2008), the various microbes involved (Rohe et al., 2014a; Sutka et al., 2003, 2008) and to estimate the fraction of N₂O reduced to N₂ (Ostrom et al., 2007; Park et al., 2011; Toyoda et al., 2011; Well and Flessa, 2009). However, the usefulness of these analyses would be enhanced further if the isotope fractionation mechanisms were better understood. In particular, we need to recognize the isotope effects associated with nitrate and N₂O reduction to quantify the entire gaseous nitrogen losses as N₂O and N₂ based on the N₂O isotopic signatures (Lewicka-Szczebak et al., 2014, 2015). This would be most effective if either of the isotopic signatures ($\delta^{18}\text{O}$, $\delta^{15}\text{N}^{\text{av}}$ or $\delta^{15}\text{N}^{\text{sp}}$) were stable or predictable for N₂O produced by each of the relevant N₂O forming processes (e.g. heterotrophic bacterial denitrification, fungal denitrification, nitrifier denitrification and nitrification). We hypothesize that this could be the case for $\delta^{18}\text{O}$, and this study aims to increase the understanding of the factors controlling $\delta^{18}\text{O}$ during N₂O production in soils.

$\delta^{18}\text{O}(\text{N}_2\text{O})$ has been rarely applied in the interpretation of N₂O isotopic signatures because of the rather complex oxygen isotope fractionations during N₂O production by denitrification (Kool et al., 2007). Denitrification is a stepwise process of nitrate reduction mediated by three enzymes: nitrate reductase (NAR), nitrite reductase (NIR) and nitric oxide reductase (NOR) (Fig. 1). $\delta^{18}\text{O}(\text{N}_2\text{O})$ is controlled by the origin of the oxygen atom in the N₂O molecule (nitrate, nitrite, soil water or molecular O₂) and by the isotope fractionation during nitrate reduction or during oxygen isotope exchange with soil water.

During each reduction step, one oxygen atom is detached and removed as water (H₂O), which is associated with branching isotope effects (Casciotti et al., 2007; Snider et al., 2013). Conceptually, these can be regarded as a combination of two isotope fractionations with opposite effects on the $\delta^{18}\text{O}$ signature of the reduction product: (i) intermolecular fractionation due to preferential reduction of ¹⁸O-depleted molecules, which results in ¹⁸O-enriched residual substrate and ¹⁸O-depleted product, and (ii) intramolecular fractionation due to preferential ¹⁶O abstraction, which results in ¹⁸O-enriched nitrogen-bearing reduction products and ¹⁸O-depleted H₂O as side product. Since intermolecular fractionation causes ¹⁸O depletion of the reduction product and intramolecular fractionation causes ¹⁸O enrichment, the net branching effect (ϵ_n), as the sum of both, can theoretically vary between negative and positive values. However, pure cultures studies show that ϵ_n is mostly positive, i.e. between 25 and 30 ‰ for bacterial denitrification (Casciotti et al., 2007) and between 10 and 30 ‰ for fungal denitrification

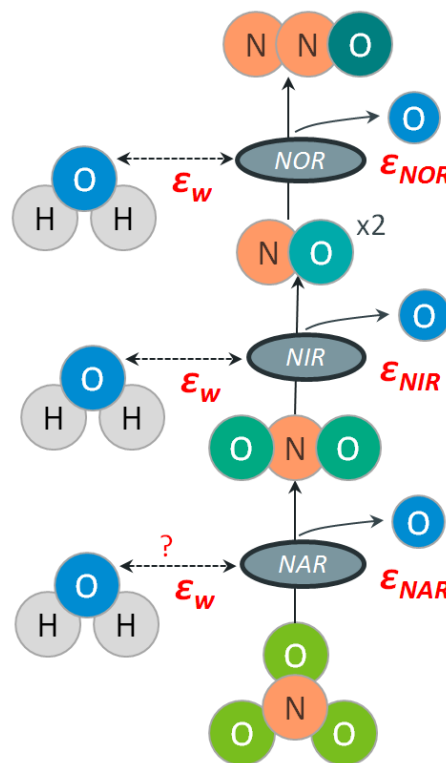


Figure 1. Oxygen isotope fractionation during denitrification as a result of branching effects (ϵ_{NAR} , ϵ_{NIR} , ϵ_{NOR}) and exchange effects (ϵ_w) associated with the following enzymatic reaction steps: NAR, NIR and NOR.

(Rohe et al., 2014a). Importantly, the intra- and intermolecular isotope effects can only manifest together during incomplete substrate consumption (Rohe et al., 2014a). In the case of complete substrate conversion, the net branching effect reflects the intramolecular effect only (Casciotti et al., 2007).

Moreover, denitrification intermediates may partially or fully exchange oxygen isotopes with ambient water (Kool et al., 2009). The isotopic signature of the incorporated O-atom depends on the isotopic signature of ambient water and the isotope fractionation associated with this exchange. Under typical soil conditions, i.e. pH close to neutral and moderate temperatures, abiotic isotope exchange between nitrate and water is negligibly slow. In extremely acid conditions (pH < 0), the equilibrium effect is $\epsilon(\text{NO}_3^- / \text{H}_2\text{O}) = 23 \text{ ‰}$ (Böhlke et al., 2003). Casciotti et al. (2007) showed that for nitrite the abiotic exchange can occur at neutral pH, but for achieving an isotopic equilibrium over 8 months are needed. The observed isotope equilibrium effect between nitrite and water is $\epsilon(\text{NO}_2^- / \text{H}_2\text{O}) = 14 \text{ ‰}$ at 21 °C. Nothing is known yet about the possible abiotic exchange between NO and ambient water. The isotope exchange between denitrification intermediates and ambient water is most probably accelerated by enzymatic catalysis, since numerous ¹⁸O tracer studies documented nearly complete O isotope exchange (Kool et

al., 2009; Rohe et al., 2014b; Snider et al., 2013) within short incubation times like a few hours. Hence, it can be assumed that at least one enzymatic step must be responsible for exchange of O isotopes with soil water (Rohe et al., 2014a; Snider et al., 2013). In pure culture studies the extent of oxygen isotope exchange ranged from 4 to 100 % for bacterial denitrification (Kool et al., 2007) and from 11 to 100 % for fungal denitrification (Rohe et al., 2014b). In contrast, unsaturated soil incubation experiments, with a natural whole microbial community, showed consistently high magnitudes of oxygen isotope exchange of between 85 and 99 % (Kool et al., 2009; Lewicka-Szczebak et al., 2014; Snider et al., 2013). If the high extent of isotope exchange was characteristic of soil denitrification processes, we would expect quite stable $\delta^{18}\text{O}$ values of the produced N₂O during denitrification.

It is difficult to quantitatively link isotope exchange and apparent isotope effects, because using the ^{18}O tracer technique to quantify isotope exchange prevents simultaneous study of isotope oxygen fractionation. However, two studies that conducted parallel ^{18}O traced and natural abundance experiments allowed formulating general oxygen isotope fractionation models (Rohe et al., 2014a; Snider et al., 2013). These models showed that the magnitude of overall isotope fractionation depends not only on the extent of oxygen isotope exchange but also on the enzymatic reduction step associated with this exchange (Fig. 1). It was found that the oxygen isotope exchange is predominantly associated with NIR for fungal denitrification (Rohe et al., 2014a). Fungi and bacteria are characterized by different NOR mechanisms (Schmidt et al., 2004; Stein and Yung, 2003), resulting in distinct $\delta^{15}\text{N}^{\text{sp}}$ values for bacterial and fungal denitrification. It is possible that these different NOR mechanisms also influence $\delta^{18}\text{O}$.

In the present study, we used ^{17}O as tracer to determine the extent of O isotope exchange, in order to investigate both isotope exchange and apparent isotope effects. We applied a nitrate fertilizer of natural atmospheric deposition origin with high ^{17}O excess, as a result of non-random oxygen isotope distribution. Then we measured ^{17}O excess of the produced N₂O and, based on the observed loss of ^{17}O excess, calculated the extent of isotope exchange with water. Simultaneously, we could measure the $^{18}\text{O}/^{16}\text{O}$ fractionation in the same incubation vessels, since the ^{17}O tracing method has no impact on $\delta^{18}\text{O}$. This is the first time that such an approach has been used. To validate this method, we applied an alternative approach – namely, soil water with distinct $\delta^{18}\text{O}$ values within the range of natural abundance isotopic signatures was applied to quantify isotope exchange (Snider et al., 2009). The latter method has also been applied in a recent soil incubation study (Lewicka-Szczebak et al., 2014) and indicated almost complete oxygen isotope exchange with soil water associated with a stable isotope ratio difference between soil water and produced N₂O of $\delta^{18}\text{O}(\text{N}_2\text{O}/\text{H}_2\text{O}) = (19.0 \pm 0.7)\%$. However, the results of other experiments presented in the same

study (Lewicka-Szczebak et al., 2014) indicated much higher $\delta^{18}\text{O}(\text{N}_2\text{O}/\text{H}_2\text{O})$ values of up to 42 %. The higher values may be due to a lower extent of oxygen isotope exchange, but no data were available regarding the extent of exchange for those samples. In the present study, we investigated possible controlling factors for oxygen isotope exchange by applying various experimental treatments differing in soil moisture and temperature.

The combination of various experimental approaches allowed us to further improve the $\delta^{18}\text{O}$ fractionation model proposed by Snider et al. (2013) and Rohe et al. (2014a), to decipher the mechanism of oxygen isotope fractionation during N₂O production by denitrification and to determine the associated isotope effects. We investigated the variability of isotope exchange with soil water and of the $\delta^{18}\text{O}$ values of produced N₂O under varying conditions as well as the relation between these quantities. Ultimately, our aim was to check to what level of accuracy $\delta^{18}\text{O}$ can be predicted based on the known controlling factors.

Additionally, the ^{17}O analyses of N₂O produced by denitrification gave us the opportunity to test the hypothesis of soil denitrification contributing to the non-random distribution of oxygen isotopes (^{17}O excess, or $\Delta^{17}\text{O}$) in atmospheric N₂O (Kaiser et al., 2004; Michalski et al., 2003).

2 Methods

2.1 Experimental set-ups

2.1.1 Experiment 1 (Exp 1) – static anoxic incubation

The static incubations were performed under an anoxic atmosphere (N₂) in closed, gas-tight vessels where denitrification products accumulated in the headspace. Two arable soil types were used: a *Luvisol* with loamy sand texture and *Haplic Luvisol* with silt loam texture with pH (in 0.01 M CaCl₂) of 5.7 and 7.4, respectively. More details on soil properties can be found in Lewicka-Szczebak et al. (2014). For the first part of these incubations (Exp 1.1) two different temperature treatments were applied (8 and 22 °C) and only one moisture treatment of 80 % WFPS (water-filled pore space). The results of $\delta^{18}\text{O}(\text{N}_2\text{O})$ analyses for these samples have already been published (Lewicka-Szczebak et al., 2014). Here we expand these data with $\Delta^{17}\text{O}(\text{N}_2\text{O})$ analyses. The second part of the static incubations (Exp 1.2) was performed for the same two soils with three different moisture treatments of 50, 65 and 80 % WFPS at one temperature (22 °C). Details on the treatments are presented as supplementary information in Supplement Table S1.

This experimental approach is described in detail in Lewicka-Szczebak et al. (2014). In short, the soil was air dried and sieved at 2 mm mesh size. Afterwards, the soil was rewetted to obtain the target WFPS and fertilized with 50 (Exp 1.1) or 10 (Exp 1.2) mg N equivalents (as NaNO₃)

per kg soil. Various nitrate and water treatments were applied (Table S1). The soils were rewetted using two waters with distinct isotopic signatures – *heavy water* ($\delta^{18}\text{O} = -1.5\text{‰}$) and *light water* ($\delta^{18}\text{O} = -14.8\text{‰}$) – and fertilized with two different nitrate fertilizers – natural *Chile saltpeter* (NaNO_3 , Chili Borium Plus, Prills-Natural origin, supplied by Yara, Dülmen, Germany, $\delta^{18}\text{O} = 56\text{‰}$) and *synthetic NaNO₃* (Sigma Aldrich, Taufkirchen, Germany, $\delta^{18}\text{O} = 27\text{‰}$). The soils were thoroughly mixed to obtain a homogeneous distribution of water and fertilizer and an equivalent of 100 g of dry soil was repacked into each incubation jar at bulk densities of 1.3 g cm^{-3} for the silt loam soil and 1.6 g cm^{-3} for the loamy sand soil. The 0.8 dm^3 jars (J. WECK GmbH u. Co. KG, Wehr, Germany) were used with airtight rubber seals and with two three-way valves installed in their glass cover to enable sampling and flushing. The jars were flushed with N₂ at approximately $500\text{ cm}^3\text{ min}^{-1}$ (STP: 273.15 K, 100 kPa) for 10 min to create anoxic conditions. Immediately after flushing, acetylene (C₂H₂) was added to inhibit N₂O reduction in selected jars (C₂H₂ inhibited treatment), by replacing 80 cm^3 of N₂ with C₂H₂, which resulted in $10\text{ kPa C}_2\text{H}_2$ in the headspace. Each treatment (Table 1) had three replicates. The soils were incubated for approximately 25 h and three to four samples were collected at 4–12 h intervals by transferring 30 cm^3 of headspace gases into two pre-evacuated 12 cm^3 Exetainer vials (Labco Limited, Ceredigion, UK). The excess 3 cm^3 of headspace gas in each vial ensured that no ambient air entered the vials. The removed sample volume was immediately replaced by pure N₂ gas.

Additional treatments with addition of ¹⁵N-labelled NaNO₃ (98 % ¹⁵N isotopic purity) were used to control the efficiency of acetylene inhibition and to determine the N₂O mole fraction $f(\text{N}_2\text{O}) = c(\text{N}_2\text{O}) / [c(\text{N}_2) + c(\text{N}_2\text{O})]$ (c : volumetric concentration) in non-inhibited treatments. This method allows determination of the N₂ concentration originating from the ¹⁵N labelled pool and hence the N₂O mole fraction (Lewicka-Szczebak et al., 2013).

2.1.2 Experiment 2 (Exp 2) – flow-through incubation under He atmosphere

The flow-through incubations were performed using a special gas-tight incubation system allowing for incubation under N₂-free atmosphere to enable direct quantification of soil N₂ fluxes (Butterbach-Bahl et al., 2002; Scholefield et al., 1997). This system has been described in detail by Eickenscheidt et al. (2014). Four different soils were incubated: two arable soils, the same as in Exp 1 (loamy sand and silt loam), and two grassland soils: an organic soil classified as *Histic Gleysol* and a sandy soil classified as *Plaggic Anthrosol*, with pH (in 0.01 M CaCl₂) of 5.9 and 5.3, respectively. All soils were incubated at the target moisture level of 80 % WFPS and the two most active soils (organic and silt loam soil)

were additionally incubated at the lower moisture level of 70 % WFPS (target values, for actual values see Table 2).

The soils were air dried and sieved at 4 mm mesh size. Afterwards, the soil was rewetted to obtain 70 % WFPS and fertilized with 50 mg N equivalents (as NaNO₃) per kg soil with natural fertilizer *Chile saltpeter*. The soils were thoroughly mixed to obtain a homogeneous distribution of water and fertilizer and 250 cm^3 of wet soil was repacked into each incubation vessel at bulk densities of 1.4 g cm^{-3} for the silt loam soil, 1.6 g cm^{-3} for the loamy sand soil, 1.5 g cm^{-3} for the sandy soil, and 0.4 g cm^{-3} for the organic soil. Afterwards, the water deficit to the target WFPS was added on the top of the soil for 80 % WFPS treatments. Each treatment had three replicates. The incubation vessels were cooled to 2 °C and repeatedly evacuated (to 4.7 kPa) and flushed with He to reduce the N₂ background and afterwards flushed with a continuous flow of 20 % O₂ in helium (He / O₂) mixture at $15\text{ cm}^3\text{ min}^{-1}$ (STP) for at least 60 h. When a stable and low-N₂ background (below $10\text{ }\mu\text{mol mol}^{-1}$) was reached, temperature was increased to 22 °C. During the incubation the headspace was constantly flushed with He / O₂ mixture (first 3 days; Part 1) and then with He (last 2 days; Part 2) at a flow rate of approximately $15\text{ cm}^3\text{ min}^{-1}$ (STP). The fluxes of N₂O and N₂ were analysed immediately (see Sect. 2.2) and $f(\text{N}_2\text{O})$ was determined. Samples for N₂O isotopocule analyses were collected by connecting the sampling vials in line with the exhaust gas of each incubation vessels and exchanging them at least twice a day. The results presented in this study originate from the anoxic Part 2 of the incubation, since the N₂O fluxes during the Part 1 were too low for $\Delta^{17}\text{O}$ analyses. The results for two samples taken approximately 8 and 24 h after switch to anoxic conditions are shown.

2.2 Gas chromatographic analyses

In Exp 1 the samples for gas concentration analyses were collected in Exetainer vials (Labco Limited, Ceredigion, UK) and were analysed using an Agilent 7890A gas chromatograph (GC) (Agilent Technologies, Santa Clara, CA, USA) equipped with an electron capture detector (ECD). Measurement repeatability as given by the relative standard deviation (1σ) of four standard gas mixtures was typically 1.5 %.

In Exp 2, online trace gas concentration analysis of N₂ was performed with a micro-GC (Agilent Technologies, 3000 Micro GC), equipped with a thermal conductivity detector (TCD) and N₂O was measured with a GC (Shimadzu, Duisburg, Germany, GC-14B) equipped with ECD detector. The measurement repeatability (1σ) was better than 0.02 for N₂O and $0.2\text{ }\mu\text{mol mol}^{-1}$ for N₂.

Table 1. Exp 1 results: soil moisture (expressed as water-filled pore space: WFPS), N₂O + N₂ production rate (expressed as mass of N as sum of N₂O and N₂ per mass of dry soil per time), ¹⁷O excess in soil nitrate ($\Delta^{17}\text{O}(\text{NO}_3^-)$) and in N₂O ($\Delta^{17}\text{O}(\text{N}_2\text{O})$) with calculated exchange with soil water (x), and oxygen isotopic signature ($\delta^{18}\text{O}$) of soil nitrate (NO_3^-), soil water (H_2O) and N₂O with calculated isotope ratio difference between soil water and N₂O ($\delta_0^{18}\text{O}(\text{N}_2\text{O}/\text{H}_2\text{O})$). For samples with non-inhibited N₂O reduction the N₂O mole fraction ($f(\text{N}_2\text{O})$) was taken into account to calculate the $\delta^{18}\text{O}$ unaffected by N₂O reduction ($\delta_0^{18}\text{O}(\text{N}_2\text{O})$) and the respective $\delta_0^{18}\text{O}(\text{N}_2\text{O}/\text{H}_2\text{O})$. Only *Chile salpeter* treatments are presented, for which the individual determination of x was possible. Part of the data from Exp 1.1 ($\delta^{18}\text{O}(\text{NO}_3^-)$, $\delta^{18}\text{O}(\text{H}_2\text{O})$, $\delta^{18}\text{O}(\text{N}_2\text{O})$) has already been published in Lewicka-Szczebak et al. (2014).

treatment		N ₂ O + N ₂ production rate ($\mu\text{g kg}^{-1} \text{h}^{-1}$)	$\Delta^{17}\text{O}(\text{NO}_3^-)$ (‰)	$\Delta^{17}\text{O}(\text{N}_2\text{O})$ (‰)	x (%)	$\delta^{18}\text{O}(\text{NO}_3^-)$ (‰)	$\delta^{18}\text{O}(\text{H}_2\text{O})$ (‰)	$\delta^{18}\text{O}(\text{N}_2\text{O})$ (‰)	$f(\text{N}_2\text{O})^a$	$\delta_0^{18}\text{O}(\text{N}_2\text{O})^b$ (‰)	$\delta_0^{18}\text{O}(\text{N}_2\text{O}/\text{H}_2\text{O})$ (‰)
WFPS (%)	inhibition (%)										
Exp 1.1 a, loamy sand, 8 °C											
80		114	11.9 ± 0.6	0.4 ± 0.5	96.2 ± 4.7	38.8 ± 0.5	-9.2 ± 0.5	13.4 ± 0.2	0.84 ± 0.04	10.4	19.7 ± 0.5
80	C ₂ H ₂	107	11.9 ± 0.6	0.8 ± 0.4	93.1 ± 3.1	38.8 ± 0.5	-9.2 ± 0.5	10.4 ± 0.1	1	10.4	19.8 ± 0.5
80		125	11.9 ± 0.6	0.8 ± 0.2	92.7 ± 1.1	37.5 ± 0.5	-13.5 ± 0.5	8.4 ± 0.3	0.84 ± 0.04	5.4	19.1 ± 0.6
80	C ₂ H ₂	126	11.9 ± 0.6	0.3 ± 0.7	96.2 ± 3.4	37.5 ± 0.5	-13.5 ± 0.5	5.7 ± 0.0	1	5.7	19.4 ± 0.5
Exp 1.1 b, loamy sand, 22 °C											
80		427	10.4 ± 0.8	0.4 ± 0.2	95.7 ± 1.8	42.6 ± 0.5	-9.2 ± 0.5	12.5 ± 0.2	0.85 ± 0.06	9.6	19.0 ± 0.5
80	C ₂ H ₂	362	10.4 ± 0.8	0.4 ± 0.0	96.4 ± 0.2	42.6 ± 0.5	-9.2 ± 0.5	9.5 ± 0.0	1	9.5	18.9 ± 0.5
80		429	10.4 ± 0.8	0.2 ± 0.1	98.2 ± 1.5	42.1 ± 0.5	-13.5 ± 0.5	7.5 ± 0.1	0.85 ± 0.06	4.7	18.4 ± 0.5
80	C ₂ H ₂	370	10.4 ± 0.8	0.5 ± 0.1	94.8 ± 0.5	42.1 ± 0.5	-13.5 ± 0.5	4.5 ± 0.1	1	4.5	18.3 ± 0.5
Exp 1.1 c, silt loam, 22 °C											
80		266	9.2 ± 1.3	0.0 ± 0.2	99.5 ± 0.9	31.8 ± 0.5	-2.6 ± 0.5	26.4 ± 0.1	0.57 ± 0.03	16.4	19.1 ± 0.5
80	C ₂ H ₂	257	9.2 ± 1.3	0.4 ± 0.1	95.3 ± 1.4	31.8 ± 0.5	-2.6 ± 0.5	15.9 ± 0.1	1	15.9	18.5 ± 0.5
80		271	9.2 ± 1.3	0.1 ± 0.2	98.6 ± 1.3	31.8 ± 0.5	-8.7 ± 0.5	20.7 ± 0.2	0.57 ± 0.03	10.8	19.7 ± 0.5
80	C ₂ H ₂	251	9.2 ± 1.3	0.4 ± 0.1	95.0 ± 1.5	31.8 ± 0.5	-8.7 ± 0.5	9.8 ± 0.1	1	9.8	18.7 ± 0.5
Exp 1.2 a, loamy sand, 22 °C											
80	C ₂ H ₂	126	3.4 ± 0.5	n.d.	n.d.	6.5 ± 0.5	-10.4 ± 0.5	6.3 ± 0.1	1	6.3	16.9 ± 0.5
65	C ₂ H ₂	112	3.4 ± 0.5	0.2 ± 0.3	92.6 ± 8.5	6.5 ± 0.5	-10.1 ± 0.5	6.9 ± 0.2	1	6.9	17.2 ± 0.5
50	C ₂ H ₂	50	3.4 ± 0.5	0.0 ± 0.3	95.8 ± 3.9	6.5 ± 0.5	-8.9 ± 0.5	7.6 ± 0.3	1	7.6	16.6 ± 0.6
80	C ₂ H ₂	161	3.4 ± 0.5	n.d.	n.d.	6.5 ± 0.5	-5.0 ± 0.5	10.5 ± 0.0	1	10.5	15.6 ± 0.5
65	C ₂ H ₂	102	3.4 ± 0.5	0.2 ± 0.2	92.7 ± 5.2	6.5 ± 0.5	-5.7 ± 0.5	11.6 ± 0.1	1	11.6	17.5 ± 0.5
50	C ₂ H ₂	74	3.4 ± 0.5	0.2 ± 0.2	94.5 ± 5.1	6.5 ± 0.5	-6.6 ± 0.5	10.7 ± 0.1	1	10.7	17.4 ± 0.5
Exp 1.2 b, silt loam, 22 °C											
80	C ₂ H ₂	137	2.6 ± 0.4	0.2 ± 0.2	90.6 ± 7.3	3.2 ± 0.5	-8.1 ± 0.5	8.3 ± 0.1	1	8.3	16.5 ± 0.5
65	C ₂ H ₂	130	2.6 ± 0.4	0.2 ± 0.1	92.2 ± 3.7	3.2 ± 0.5	-7.1 ± 0.5	9.8 ± 0.1	1	9.8	17.1 ± 0.5
50	C ₂ H ₂	121	2.6 ± 0.4	0.1 ± 0.1	96.5 ± 4.3	3.2 ± 0.5	-5.9 ± 0.5	12.5 ± 0.2	1	12.5	18.6 ± 0.5
80	C ₂ H ₂	111	2.6 ± 0.4	-0.1 ± 0.1	99.1 ± 1.6	3.2 ± 0.5	-1.6 ± 0.5	15.1 ± 0.2	1	15.1	16.7 ± 0.6
65	C ₂ H ₂	132	2.6 ± 0.4	0.0 ± 0.1	98.4 ± 1.6	3.2 ± 0.5	-1.8 ± 0.5	15.2 ± 0.2	1	15.2	17.0 ± 0.5
50	C ₂ H ₂	106	2.6 ± 0.4	-0.2 ± 0.0	100.0 ± 1.8	3.2 ± 0.5	-2.0 ± 0.5	15.7 ± 0.3	1	15.7	17.7 ± 0.6

^a $c(\text{N}_2\text{O})/[c(\text{N}_2) + c(\text{N}_2\text{O})]$; based on parallel ¹⁵N treatment (last sampling results). Where ^b N₂O reduction not inhibited, the values are corrected taking into account product ratio and isotope fractionation, according to Rayleigh fractionation $^{18}\text{O}(\text{N}_2/\text{N}_2\text{O})$ values taken from Lewicka-Szczebak et al. (2014): -17.4‰ (see Sect. 2.5 for details).

2.3 Isotopic analyses

2.3.1 Isotopocules of N₂O

Gas samples were analysed using a Delta V isotope ratio mass spectrometer (Thermo Scientific, Bremen, Germany) coupled to automatic preparation system: Precon + Trace GC Isolink (Thermo Scientific, Bremen, Germany) where N₂O was preconcentrated, separated and purified. In the mass spectrometer, N₂O isotopocule signatures were determined by measuring m/z 44, 45 and 46 of intact N₂O⁺ ions as well as m/z 30 and 31 of NO⁺ fragments ions. This allows the determination of average $\delta^{15}\text{N}^{\text{av}}$, $\delta^{15}\text{N}^{\alpha}$ ($\delta^{15}\text{N}$ of the central N position of the N₂O molecule) and $\delta^{18}\text{O}$ (Toyoda and Yoshida, 1999). $\delta^{15}\text{N}^{\beta}$ ($\delta^{15}\text{N}$ of the peripheral N position of the N₂O molecule) is calculated using $\delta^{15}\text{N}^{\text{av}} = (\delta^{15}\text{N}^{\alpha} +$

$\delta^{15}\text{N}^{\beta})/2$. The ¹⁵N site preference ($\delta^{15}\text{N}^{\text{sp}}$) is defined as $\delta^{15}\text{N}^{\text{sp}} = \delta^{15}\text{N}^{\alpha} - \delta^{15}\text{N}^{\beta}$. The scrambling factor and ¹⁷O-correction were taken into account (Kaiser and Röckmann, 2008; Röckmann et al., 2003). Pure N₂O (Westfalen, Münster, Germany) was used as internal reference gas and was analysed in the laboratory of the Tokyo Institute of Technology using calibration procedures reported previously (Toyoda and Yoshida, 1999; Westley et al., 2007). Moreover, the comparison materials from an intercalibration study (S1, S2) were used to perform a two-point calibration (Mohn et al., 2014). For correction of non-linear effect due to variable sample amount five different standard gas mole fractions (0.3, 1, 5, 10, 20 $\mu\text{mol mol}^{-1}$) were analysed in each sample run. Samples with similar N₂O mole fractions were run together with at least two standard gases with similar mole fractions.

Table 2. Exp 2 results: soil moisture (expressed as water-filled pore space: WFPS), N₂O+N₂ production rate (expressed as mass of N as sum of N₂O and N₂ per mass of dry soil per time), ¹⁷O excess in soil nitrate (Δ¹⁷O(NO₃⁻)) and in N₂O (Δ¹⁷O(N₂O)) with calculated exchange with soil water (*x*) and oxygen isotopic signature (δ¹⁸O) of soil nitrate (NO₃⁻), soil water (H₂O) and N₂O. All δ¹⁸O(N₂O) values were corrected taking into account N₂O mole fraction (*f*(N₂O)) to calculate the values unaffected by N₂O reduction (δ₀¹⁸O(N₂O)) and the respective δ₀¹⁸O(N₂O / H₂O).

WFPS (%)	N ₂ O+N ₂ production rate (μg kg ⁻¹ h ⁻¹)	Δ ¹⁷ O(NO ₃ ⁻) (‰)	Δ ¹⁷ O(N ₂ O) (‰)	<i>x</i> (%)	δ ¹⁸ O(NO ₃ ⁻) (‰)	δ ¹⁸ O(H ₂ O) (‰)	δ ¹⁸ O(N ₂ O) (‰)	<i>f</i> (N ₂ O) ^a	δ ₀ ¹⁸ O (N ₂ O) ^b (‰)	δ ₀ ¹⁸ O (N ₂ O / H ₂ O) (‰)
Exp 2.1, sand 73.6±0.7	91	10.8±0.3	2.7±0.4 2.6±1.1	73.9±4.2 74.4±11.0	34.3±1.7	-8.6±0.5	12.1±0.2 11.0±0.4	0.95±0.01 0.92±0.01	11.5±0.2 10.0±0.5	20.2±0.5 18.8±0.7
Exp 2.2 loamy sand 70.4±0.9	49	11.9±0.3	3.7±0.4 3.3±0.2	66.9±3.1 71.2±1.6	43.0±2.4	-7.4±0.5	18.4±2.7 15.7±0.9	0.80±0.05 0.83±0.02	15.7±2.1 13.5±0.7	23.3±2.2 21.0±0.8
Exp 2.3 silt loam 78.4±1.9	80	11.3±0.2	5.2±0.2 5.3±0.1	52.0±2.2 50.4±1.4	43.1±2.3	-5.3±0.5	43.8±2.2 46.1±3.9	0.32±0.03 0.29±0.10	29.4±2.6 30.4±0.2	34.9±2.6 35.9±0.5
Exp 2.4 silt loam 73.6±1.8	52	12.1±0.3	3.5±0.5 5.0±0.5	69.9±4.0 56.3±4.1	52.0±3.3	-5.0±0.5	30.1±0.4 37.7±4.1	0.68±0.02 0.63±0.07	25.4±0.7 31.9±4.3	30.5±0.9 37.1±4.3
Exp 2.5 organic 86.5±1.8	743	7.8±0.2	2.3±1.1 2.3±0.8	68.1±13.8 68.2±9.5	30.4±0.6	-6.4±0.5	26.4±5.3 37.7±2.9	0.60±0.02 0.51±0.02	20.0±5.1 29.3±3.3	26.6±5.1 36.0±3.3
Exp 2.6 organic 78.7±0.4	1198	12.5±0.7	1.1±0.2 2.3±0.3	90.2±1.8 78.8±3.0	43.6±5.6	-6.7±0.5	18.5±0.0 25.6±0.8	0.82±0.02 0.74±0.05	16.1±0.2 21.9±1.6	22.9±0.6 28.7±1.7

^a $c(\text{N}_2\text{O}) / [c(\text{N}_2) + c(\text{N}_2\text{O})]$; based on direct GC measurements in N₂-free atmosphere. ^b initial δ¹⁸O values of unreduced N₂O calculated according to Rayleigh fractionation. ¹⁸ε(N₂ / N₂O) values taken from Lewicka-Szczebak et al. (2015): -12‰ (see Sect. 2.5).

All isotopic signatures are expressed as relative deviation (in ‰) from the ¹⁵N / ¹⁴N, ¹⁷O / ¹⁶O and ¹⁸O / ¹⁶O ratios of the reference materials (i.e. atmospheric N₂ and Vienna Standard Mean Ocean Water (VSMOW), respectively). The measurement repeatability (1σ) of the internal standard (filled into vials and measured in the same way as the samples) for measurements of δ¹⁵N^{av}, δ¹⁸O and δ¹⁵N^{sp} was typically 0.1, 0.1 and 0.5 ‰, respectively.

2.3.2 δ¹⁸O of NO₃⁻

Soil nitrate was extracted in 0.01 M aqueous CaCl₂ solution (soil : solution weight ratio of 1 : 10) by shaking at room temperature for 1 h. δ¹⁸O of nitrate in the soil solution was determined using the bacterial denitrification method Casciotti et al., 2002). The measurement repeatability (1σ) of the international standards (USGS34, USGS35, IAEA-NO-3) was typically 0.5 ‰ for δ¹⁸O.

2.3.3 Δ¹⁷O excess in N₂O and NO₃⁻

N₂O samples collected from soil incubation and N₂O produced from soil NO₃⁻ by the bacterial denitrifier method were analysed for Δ¹⁷O using the thermal decomposition method (Kaiser et al., 2007) with a gold oven (Exp 1.1b, c and 1.2a, b) and with a gold-wire oven (Exp 1.1a and 2) (Dyckmans et al., 2015). The ¹⁷O excess, Δ¹⁷O, is defined as (Kaiser et al., 2007)

$$\Delta^{17}\text{O} = \frac{1 + \delta^{17}\text{O}}{(1 + \delta^{18}\text{O})^{0.5279}} - 1. \quad (1)$$

The measurement repeatability (1σ) of the international standards (USGS34, USGS35) was typically 0.5 ‰ for Δ¹⁷O.

2.3.4 Soil water analyses

Soil water was extracted with the method described by Königer et al. (2011) and δ¹⁸O of water samples (with respect to VSMOW) was measured using cavity ring-down spectrometer Picarro L1115-*i* (Picarro Inc., Santa Clara, USA). The measurement repeatability (1σ) of the internal standards (three calibrated waters with known δ¹⁸O: -19.67, -8.60, +1.37 ‰) was below 0.1 ‰. The overall error associated with the soil water extraction method determined as standard deviation (1σ) of the five sample replicates was below 0.5 ‰.

2.4 Determination of the extent of isotope exchange

The extent of isotope exchange (*x*) was determined with two independent methods described below. In Exp 1 both approaches were applied simultaneously on the same soil samples, which allowed quantifying the oxygen isotope exchange with two different methods independently. This enabled the validation of the ¹⁷O excess method, which was used here for the first time for quantification of isotope exchange. Afterwards this validated method was applied in the following Exp 2. For both presented methods it is assumed that after N₂O is formed, no further oxygen isotope exchange with H₂O occurs.

2.4.1 $\delta^{18}\text{O}$ method

This method determines the isotope exchange based on the relative difference between $\delta^{18}\text{O}$ of produced N₂O and its potential precursors: soil water and soil nitrate (Snider et al., 2009). To make this method applicable, parallel incubations with distinct water and/or nitrate isotopic signatures must be carried out. Therefore, treatments with different water and nitrate isotopic signatures were applied in Exp 1 (Tables 1, S1). The calculation is based on two end-member mixing model (water (δ_w) and nitrate (δ_n); δ stands for $\delta^{18}\text{O}(\text{N}_2\text{O})$) taking into account the isotope fractionation associated with O atom incorporation into N₂O from each end-member (ε_w , fractionation associated with oxygen isotope exchange with water; ε_n , fractionation associated with branching effect during nitrate reduction). This is expressed as

$$1 + \delta = x(1 + \delta_w)(1 + \varepsilon_w) + (1 - x)(1 + \delta_n)(1 + \varepsilon_n) \quad (2)$$

which can be rearranged to

$$\frac{\delta - \delta_n}{1 + \delta_n} = x(1 + \varepsilon_w) \frac{\delta_w - \delta_n}{1 + \delta_n} + x\varepsilon_w + (1 - x)\varepsilon_n, \quad (3)$$

where $\frac{\delta - \delta_n}{1 + \delta_n} = \delta^{18}\text{O}(\text{N}_2\text{O}/\text{NO}_3^-)$ is the dependent variable of the linear regression, $\frac{\delta_w - \delta_n}{1 + \delta_n} = \delta^{18}\text{O}(\text{H}_2\text{O}/\text{NO}_3^-)$ is the independent variable of the linear regression, $x(1 + \varepsilon_w)$ is the slope of the linear regression, approximately equal to the magnitude of isotope exchange (x), and $x\varepsilon_w + (1 - x)\varepsilon_n$ is the intercept of the linear regression approximately equal to total fractionation (ε).

Hence, from the linear correlation between $\delta^{18}\text{O}(\text{N}_2\text{O}/\text{NO}_3^-)$ and $\delta^{18}\text{O}(\text{H}_2\text{O}/\text{NO}_3^-)$ we can approximate x (the deviation from the exact value may be up to 0.02, for $\varepsilon_w < 20\%$) and the total fractionation ε comprised of both ε_w and ε_n .

2.4.2 $\Delta^{17}\text{O}$ method

This method determines the isotope exchange based on the comparison of $\Delta^{17}\text{O}$ in soil nitrate and produced N₂O. It requires the application of nitrate characterized by high $\Delta^{17}\text{O}$. Therefore, soils were amended with natural NaNO₃ *Chile saltpeter* showing high $\Delta^{17}\text{O}$ (ca. 20 ‰) and the $\Delta^{17}\text{O}$ of the N₂O product was measured. $\Delta^{17}\text{O}$ of soil water was assumed to be 0 ‰.

The magnitude of oxygen isotope exchange (x) was calculated as

$$x = 1 - \frac{\Delta^{17}\text{O}(\text{N}_2\text{O})}{\Delta^{17}\text{O}(\text{NO}_3^-)}. \quad (4)$$

The error due to the use of the power-law definition of $\Delta^{17}\text{O}$ in combination with a linear mixing relationship (Eq. 4) causes a negligible relative bias of < 1 % for x .

2.5 Correction for N₂O reduction

Since $\delta^{18}\text{O}(\text{N}_2\text{O})$ values of emitted N₂O are strongly affected by partial N₂O reduction, the measured isotope values can only be informative for the mechanism of N₂O production if the reduction is inhibited or the isotope effects associated with reduction are taken into account. Exp 1, where we applied both C₂H₂-inhibited as well as uninhibited treatments (Table 1), allows us to check the validity of our correction methods as it directly yields the impact of N₂O reduction on the measured $\delta^{18}\text{O}(\text{N}_2\text{O})$ values. In Exp 2, reduction was not inhibited and the mathematical correction described below was applied.

The correction was made using the Rayleigh fractionation equation (Mariotti et al., 1981)

$$\frac{1 + \delta_S}{1 + \delta_{S0}} = f^\varepsilon, \quad (5)$$

where δ_S is the isotopic signature of the remaining substrate (here, measured $\delta^{18}\text{O}$ of the final, partially reduced, N₂O), δ_{S0} is the initial isotopic signature of the substrate (here, $\delta^{18}\text{O}$ of the produced N₂O unaffected by the reduction ($\delta_0^{18}\text{O}$); to be calculated), f is the remaining unreacted fraction (here, the N₂O mole fraction $f(\text{N}_2\text{O})$, directly measured), and ε is the isotope effect between product and substrate (here, $\varepsilon(\text{N}_2/\text{N}_2\text{O})$, the isotope effect associated with N₂O reduction, taken from the literature; Lewicka-Szczebak et al., 2014). As it has been shown that the experimental approach largely influences O isotope effect during reduction (Lewicka-Szczebak et al., 2014, 2015), we used different $\varepsilon^{18}\text{O}(\text{N}_2/\text{N}_2\text{O})$ values for static and flow-through incubations. For the static Exp 1 a mean $\varepsilon^{18}\text{O}(\text{N}_2/\text{N}_2\text{O})$ value of -17.4% is used, based on one common experiment between the study of Lewicka-Szczebak et al. (2014) (Exp 1) and this study (Exp 1.1). For the flow-through Exp 2 we accept the $\varepsilon^{18}\text{O}(\text{N}_2/\text{N}_2\text{O})$ value of -12% recently determined for similar flow-through experiments under He/O₂ atmosphere (Lewicka-Szczebak et al., 2015). For the correction of $\delta^{15}\text{N}^{\text{sp}}$ values one common $\varepsilon^{15}\text{N}^{\text{sp}}(\text{N}_2/\text{N}_2\text{O})$ value of -5% was used, since it was shown that this value is applicable for all experimental setups (Lewicka-Szczebak et al., 2014). The error due to the simplified use of $\varepsilon^{15}\text{N}^{\text{sp}}$ for the Rayleigh model (Eq. 5) instead of separate calculations with $\varepsilon^{15}\text{N}^\alpha$ and $\varepsilon^{15}\text{N}^\beta$, causes a negligible bias of the calculated $\delta_0^{15}\text{N}^{\text{sp}}$ values of < 0.15 ‰ for the presented data set.

2.6 N₂O isotopic signatures related to water

Relative isotope ratio differences between N₂O and soil water, $\delta^{18}\text{O}(\text{N}_2\text{O}/\text{H}_2\text{O})$, were calculated as the difference between the measured $\delta^{18}\text{O}$ of produced N₂O and of soil water:

$$\delta^{18}\text{O}(\text{N}_2\text{O}/\text{H}_2\text{O}) = \frac{\delta^{18}\text{O}(\text{N}_2\text{O}) - \delta^{18}\text{O}(\text{H}_2\text{O})}{1 + \delta^{18}\text{O}(\text{H}_2\text{O})} \quad (6)$$

In samples where N₂O reduction occurred $\delta^{18}\text{O}(\text{N}_2\text{O} / \text{H}_2\text{O})$ values were corrected as described above (Sect. 2.5) and for statistical analyses and modelling exercises the reduction-corrected values were used ($\delta_0^{18}\text{O}(\text{N}_2\text{O} / \text{H}_2\text{O})$).

2.7 Statistical methods

For results comparisons, an analysis of variance was used with the significance level α of 0.05. The uncertainty values provided for the measured parameters represent the standard deviation (1σ) of the replicates. The propagated uncertainty was calculated using Gauss' error propagation equation taking into account standard deviations of all individual parameters.

3 Results and discussion

3.1 Experiment 1

In Table 1 the results are presented as average values from three replicated incubation vessels with respective standard deviation. Soil nitrate and water were analysed at the beginning of the experiment from the prepared homogenized soils, hence no standard deviation but the standard analytical uncertainty is given.

For different temperature treatments, x (determined by the $\Delta^{17}\text{O}$ method) was not significantly different ($p = 0.19$) but $\delta_0^{18}\text{O}(\text{N}_2\text{O} / \text{H}_2\text{O})$ was slightly higher ($p = 0.009$) for 8 °C ($(19.5 \pm 0.3)\text{‰}$) than for 22 °C ($(18.6 \pm 0.3)\text{‰}$) treatment. No significant differences were observed between the two analysed soil types or between various soil moisture levels.

When comparing Exp 1.1 and 1.2, x did not show any significant differences, but the $\delta_0^{18}\text{O}(\text{N}_2\text{O} / \text{H}_2\text{O})$ values were significantly different ($p < 0.001$) with higher values for Exp 1.1 ($(19.1 \pm 0.5)\text{‰}$) than for Exp 1.2 ($(16.9 \pm 0.8)\text{‰}$). It should be noted that the $\delta^{18}\text{O}$ values of soil nitrate were much lower in Exp 1.2 (from -2.0 to 6.5‰) when compared to Exp 1.1 (from 31.8 to 42.6‰) which might have affected the observed differences in $\delta_0^{18}\text{O}(\text{N}_2\text{O} / \text{H}_2\text{O})$.

Moreover, for Exp 1 the $\delta^{18}\text{O}$ method was applied to estimate x and ε from the relationship between $\delta^{18}\text{O}(\text{N}_2\text{O} / \text{NO}_3^-)$ and $\delta^{18}\text{O}(\text{H}_2\text{O} / \text{NO}_3^-)$ as described in Sect. 2.4.1.

According to this method, from the linear regression one can decipher x (slope) and ε (intercept) (Snider et al., 2009). The correlation is excellent (R^2 from 0.989 to 0.997) which indicates that the x and ε are very stable for all the treatments (Fig. 2). The x is about 1 (complete exchange) and ε varies from 17.1 (Exp 1.2) to 18.2 ‰ (Exp 1.1). When compared to the results presented in Table 1, we see slightly higher isotope exchange with the $\delta^{18}\text{O}$ method when compared to the $\Delta^{17}\text{O}$ method. This may be partially due to the fact that the slope in the $\delta^{18}\text{O}$ method (Fig. 2) is actually slightly higher than x (from Eq. (3): $x(1+\varepsilon_w)$). The difference between the two experiments is mostly within the error of each method; so far

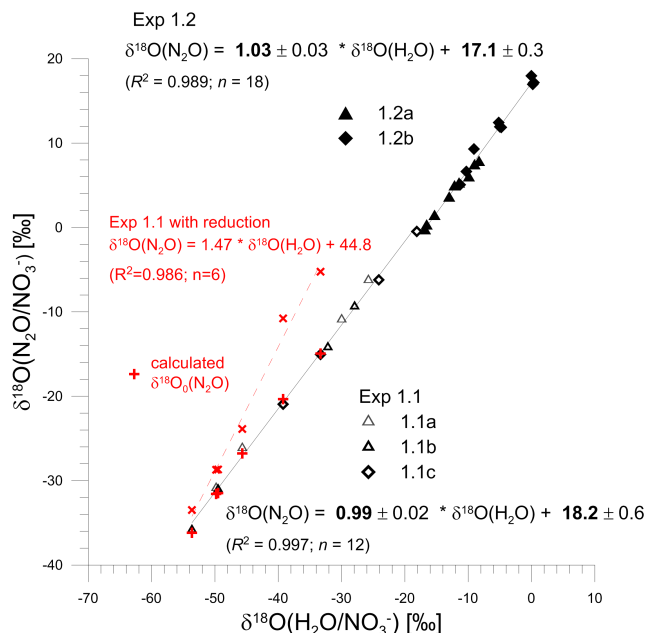


Figure 2. Correlation between oxygen isotopic signatures of N₂O and soil water expressed in relation to soil nitrate, the equation of linear fit allows for estimation of isotope exchange with soil water (slope of the linear fit) and the associated isotope effect (intercept of the linear fit). In red the influence of N₂O reduction on the method performance is presented – red “X” points represent the samples with not inhibited N₂O reduction (note that the slope and intercept are very different), whereas the red “+” points stand for the same samples after mathematical correction of N₂O reduction effect (as described in Sect. 2.5) which fit very well to the samples where N₂O reduction was inhibited. Data from Exp 1.

the results are consistent. The $\Delta^{17}\text{O}$ method is more useful, since it allows for individual determinations of x , whereas the correlation obtained from the $\delta^{18}\text{O}$ method is based on all data, hence provides a mean result for x and ε for a whole experiment.

Importantly, we found that the $\delta^{18}\text{O}$ method is not applicable to samples with uninhibited N₂O reduction, if $\delta^{18}\text{O}(\text{N}_2\text{O})$ values are not corrected for N₂O reduction. The treatment with uninhibited reduction of Exp 1.1 was tested and provided very different results, i.e. largely overestimated x (1.5) and ε (44.8) (red dashed fit line, Fig. 2). Hence, for proper determination of these factors the results from treatments with inhibited N₂O reduction were used (solid black fit line, Fig. 2). However, the $\delta^{18}\text{O}$ values after mathematical correction for N₂O reduction (red “+” points, Fig. 2) fitted very well to the correlation found for inhibited samples. Hence, the reduction corrected values ($\delta_0^{18}\text{O}(\text{N}_2\text{O})$) should rather be used when applying this method in experiments with uninhibited N₂O reduction. Moreover, in both static experiments we used the C₂H₂ inhibition technique, and our results indicate almost complete exchange of oxygen isotopes with soil

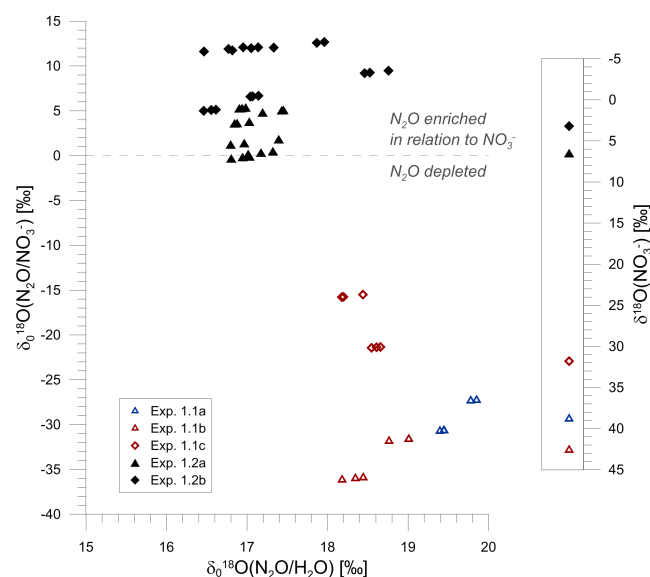


Figure 3. Relation between relative isotope ratio differences between produced N₂O and soil water ($\delta_0^{18}\text{O}(\text{N}_2\text{O}/\text{H}_2\text{O})$) and between produced N₂O and soil nitrate ($\delta_0^{18}\text{O}(\text{N}_2\text{O}/\text{NO}_3^-)$); on the right $\delta^{18}\text{O}$ values of the initial soil nitrate for different treatments. $\delta^{18}\text{O}$ values of the initial soil water ranged between -13.5 and -1.6 ‰ (see Table 1) and its variation had no impact on $\delta_0^{18}\text{O}(\text{N}_2\text{O}/\text{H}_2\text{O})$. Open symbols: treatments with synthetic nitrate as fertilizer, filled symbols: treatments with natural *Chile saltpeter* as fertilizer. Data from Exp 1.

water, which indicates that the isotope exchange process is not inhibited by C₂H₂ addition.

3.2 Experiment 2

In Table 2 the results are presented as average values from three replicate incubation vessels with respective standard deviation. The extent of oxygen isotope exchange (x) ranges from 55 to 85 % and is lower and much more variable when compared to Exp 1. $\delta_0^{18}\text{O}(\text{N}_2\text{O}/\text{H}_2\text{O})$ varies between 18.6 and 36.9 ‰, which is significantly higher when compared to the values determined in Exp 1.

3.3 Oxygen isotope effects at nearly complete isotope exchange

In the case of very high, almost complete, isotope exchange with soil water (Exp 1), the relative isotope ratio difference between N₂O and H₂O ($\delta_0^{18}\text{O}(\text{N}_2\text{O}/\text{H}_2\text{O})$) is quite stable and ranges from 15.6 to 19.8 ‰ (Table 1). In contrast, the relative isotope ratio difference between N₂O and NO₃⁻ ($\delta_0^{18}\text{O}(\text{N}_2\text{O}/\text{NO}_3^-)$) shows large variations from -36.1 to 18.0 ‰ (Fig. 3).

The ε determined in Fig. 2 represents theoretically the total oxygen isotope fractionation (from Eq. (3): $x\varepsilon_w + (1-x)\varepsilon_n$), but in the case of the nearly whole isotope ex-

change ($x = 1$) ε equals ε_w and $\varepsilon_w = (\delta_{\text{N}_2\text{O}} - \delta_w) / (\delta_w + 1) = \delta^{18}\text{O}(\text{N}_2\text{O}/\text{H}_2\text{O})$, hence both the intercept in Fig. 2 and $\delta^{18}\text{O}(\text{N}_2\text{O}/\text{H}_2\text{O})$ in Fig. 3 should provide rough estimates for ε_w . However, for $x < 1$ $\delta^{18}\text{O}(\text{N}_2\text{O}/\text{H}_2\text{O})$ depends also on δ_n and ε_n and the intercept (Fig. 2) includes ε_n . Both these values indicate a slight difference between both experiments: for Exp 1.1 ε of (18.2 ± 0.6) (intercept, Fig. 2) and $\delta^{18}\text{O}(\text{N}_2\text{O}/\text{H}_2\text{O})$ of (19.1 ± 0.5) (mean \pm SD, Table 1) are higher than for Exp 1.2, (17.1 ± 0.3) and (16.7 ± 0.8) , respectively. This slight difference is most probably due to x slightly lower than 1, as indicated by $\Delta^{17}\text{O}$ method and additional impact of δ_n and ε_n . It can be noted that $\delta_0^{18}\text{O}(\text{N}_2\text{O}/\text{H}_2\text{O})$ slightly increases with higher $\delta^{18}\text{O}$ values of nitrate (Fig. 3), i.e. the difference of about 40 ‰ in $\delta^{18}\text{O}$ of applied NO₃⁻ results in about 2 ‰ change in $\delta_0^{18}\text{O}(\text{N}_2\text{O}/\text{H}_2\text{O})$. Hence, only about 5 % of the difference in nitrate isotopic signature is reflected in the produced N₂O, suggesting that an equivalent percentage of O(N₂O) originated from NO₃⁻. This is very consistent with the determined extent of isotope exchange with soil water, which was (95.6 ± 2.6) % (Table 1).

Taken together, the data indicate that the $\delta^{18}\text{O}(\text{N}_2\text{O})$ values are clearly influenced by the $\delta^{18}\text{O}$ of soil water, whereas $\delta^{18}\text{O}$ of soil nitrates has only very little influence. Hence, the O isotope fractionation during N₂O production by denitrification should be considered in relation to soil water, rather than soil nitrates.

3.4 Oxygen isotope effects at variable isotope exchange

In contrast to Sect. 3.3, x was more variable for the flow-through incubation (Exp 2) and also significantly lower. In general, lower x was associated with higher $\delta_0^{18}\text{O}(\text{N}_2\text{O}/\text{H}_2\text{O})$ values. In Fig. 4 we can compare results from static incubations (red symbols) with the flow-through incubations (black symbols). This comparison clearly shows that the pattern of isotope exchange and associated oxygen fractionation differs significantly between both experimental approaches. The essential difference in Exp 2 was the use of a flow-through system with an oxic atmosphere at the beginning of the incubation (though results presented originate from the anoxic phase). This resulted in lower production rates for N₂O when comparing the respective soil (Tables 1 and 2), e.g. $80 \mu\text{g kg}^{-1} \text{h}^{-1}$ (mass of N as sum of N₂O and N₂ per mass of dry soil) for the silt loam soil at 80 % WFPS in Exp 2.3 but $261 \mu\text{g kg}^{-1} \text{h}^{-1}$ in Exp 1.1c. This may suggest an impact of N₂O production rate on extent of isotope exchange. However, for static anoxic incubations the effect of production rate was not observed, e.g. between Exp 1.1a and 1.1b (Table 1), where we have different production rates but similar x and $\delta_0^{18}\text{O}(\text{N}_2\text{O}/\text{H}_2\text{O})$.

Interestingly, the correlation between x and $\delta_0^{18}\text{O}(\text{N}_2\text{O}/\text{H}_2\text{O})$ seems to differ for different soil types. Very clearly both sandy soils represent distinct and weaker correlation when compared to silt loam and organic soil.

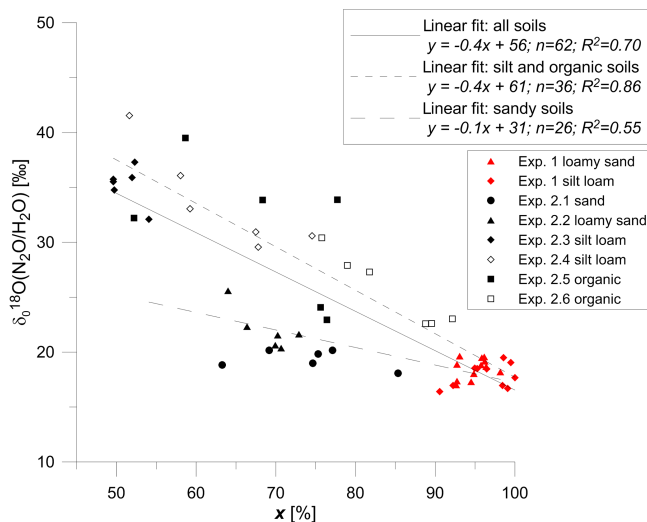


Figure 4. $\delta_0^{18}\text{O}(\text{N}_2\text{O}/\text{H}_2\text{O})$ as a function of isotope exchange extent, x (determined with $\Delta^{17}\text{O}$ method). Red symbols: Exp 1, black symbols: Exp 2; open symbols: incubations with lower WFPS (70 %), filled symbols: incubations with higher WFPS (80 %). Note that same symbol shapes always represent the same soil.

Most probably this is due to different oxygen fractionation pattern during N₂O formation in both soils, which we try to elucidate in the theoretical model presented below.

3.5 The mechanism of oxygen isotope fractionation – a fractionation model

To better understand the mechanism of oxygen isotope fractionation and the relation between the apparent isotope effect and the extent of isotope exchange we applied a simulation calculation where the total isotope effect was calculated from the theoretical isotope fractionation associated with two enzymatic reduction steps: NIR and NOR. This model was based on the calculations presented by Rohe et al. (2014a) for pure fungal cultures, where this approach has been described in detail. The model assumes that $\delta^{18}\text{O}(\text{N}_2\text{O})$ is determined by two isotope fractionation processes associated (i) with the branching isotope effect (ε_n) and (ii) with the isotope effect due to isotope exchange with soil water (ε_w), both possible at NIR or NOR. This can be expressed by the following isotope mass balance equations:

$$1 + \delta = x_{\text{NOR}}(1 + \delta_w)(1 + \varepsilon_w) + (1 - x_{\text{NOR}})(1 + \delta_{\text{NO}})(1 + \varepsilon_{\text{NOR}}) \quad (7)$$

$$1 + \delta_{\text{NO}} = x_{\text{NIR}}(1 + \delta_w)(1 + \varepsilon_w) + (1 - x_{\text{NIR}})(1 + \delta_n)(1 + \varepsilon_{\text{NIR}}), \quad (8)$$

where

$$1 - x = (1 - x_{\text{NIR}})(1 - x_{\text{NOR}}) \quad (9)$$

$$1 + \varepsilon_n = (1 + \varepsilon_{\text{NIR}})(1 + \varepsilon_{\text{NOR}}). \quad (10)$$

Table 3. Isotopic fractionation factors calculated based on Exp 1 results with Eq. (12) (see text for details). Results presented separately for Exp 1.1 and 1.2 and mean values for both.

	ε_w (‰)	ε_n (‰)
Exp 1.1	17.44 ± 0.71	0.74 ± 0.70
Exp 1.2	17.50 ± 0.67	-0.39 ± 0.66
mean all	17.48 ± 0.66	0.03 ± 0.86

After substitution and transformation, this gives

$$\frac{\delta - \delta_w}{1 + \delta_w} = \frac{(1 - x)(1 + \varepsilon_n) \frac{\delta_n - \delta_w}{1 + \delta_w} + (x - x_{\text{NOR}}) \varepsilon_{\text{NOR}}(1 + \varepsilon_w) + x\varepsilon_w + (1 - x)\varepsilon_n}{\varepsilon_{\text{NOR}}(1 + \varepsilon_w) + x\varepsilon_w + (1 - x)\varepsilon_n} \quad (11)$$

We neglected the possible fractionation associated with the NAR reduction, i.e. $\delta(\text{NO}_2^-) = \delta(\text{NO}_3^-) = \delta_n$ in Eq. (11). This enzymatic step was investigated by Rohe et al. (2014a), and appeared to have no significant impact on the total oxygen fractionation, i.e. the branching fractionation for nitrate treatments was in no case higher than for nitrite treatment. This indicates that the oxygen fractionation between nitrate and nitrite is low due to cancellation of the intramolecular effect of about 30 ‰ (Casciotti et al., 2007) by the intermolecular effect when the nitrate pool is not completely consumed. Hence, we only focused here on differentiating between NIR and NOR enzymatic reduction steps, which are most likely the enzymatic reactions crucial for determining final N₂O isotopic values (Kool et al., 2007).

There are many unknown factors in Eq. (11); first of all, isotopic fractionation factors ε_n and ε_w . We have compiled the results of both methods applied for Exp 1 data – the $\delta^{18}\text{O}$ method and the $\Delta^{17}\text{O}$ method – to estimate these factors. Using the $\delta^{18}\text{O}$ method, ε was determined from the intercept in Fig. 2 and this value represents total fractionation: $\varepsilon = x\varepsilon_w + (1 - x)\varepsilon_n$ (see Sect. 2.4.1). Using the $\Delta^{17}\text{O}$ method, individual x values were calculated for each sample. We have also measured $\delta^{18}\text{O}(\text{N}_2\text{O}/\text{H}_2\text{O})$ and $\delta^{18}\text{O}(\text{NO}_3^-/\text{H}_2\text{O})$ for each sample, hence from the transformed Eq. (3):

$$\frac{\delta - \delta_w}{1 + \delta_w} = (1 - x)(1 + \varepsilon_n) \frac{\delta_n - \delta_w}{1 + \delta_w} + x\varepsilon_w + (1 - x)\varepsilon_n \quad (12)$$

and knowing that $x\varepsilon_w + (1 - x)\varepsilon_n = 0.0182$ for Exp 1.1 and $x\varepsilon_w + (1 - x)\varepsilon_n = 0.0171$ for Exp 1.2 (Fig. 2) we have calculated ε_w and ε_n for each sample. Table 3 summarizes the results.

The determination of ε_w is very precise, with no significant difference between Exp 1.1 and 1.2 ($p = 0.868$). The value obtained (17.5 ± 0.7) ‰ is within the range of the previous values determined for chemical exchange $\varepsilon(\text{NO}_2^-/\text{H}_2\text{O}) = 14$ ‰ and $\varepsilon(\text{NO}_3^-/\text{H}_2\text{O}) = 23$ ‰ (Böhlke et al., 2003; Casciotti et al., 2007). So far there are no data for the isotope effect of chemical exchange $\varepsilon(\text{NO}/\text{H}_2\text{O})$. Therefore, we assumed equal ε_w values for isotope exchange

associated with NIR and NOR, similarly to previous studies (Rohe et al., 2014a; Snider et al., 2012). Hence, the ε_w value determined here is a hypothetical mean value of enzymatically mediated isotope exchange associated with NIR ($\varepsilon_w(\text{NO}_2^- / \text{H}_2\text{O})$) and NOR ($\varepsilon_w(\text{NO} / \text{H}_2\text{O})$).

The ε_n is also quite stable with a weak ($p = 0.006$) and very small (below 1‰) difference between Exp 1.1 and 1.2. The ε_n values found are very low and vary around 0, from -1.9 to 2.1 ‰. This is much lower than in previous studies, which reported ε_n from 10 to 30‰ (Casciotti et al., 2007; Rohe et al., 2014a).

We checked how well these calculated values fit for the individual samples of both experiments. We started with the simplest Scenario 0, where we assume the values determined in Table 3 for ε_w and ε_n and calculate the $\delta^{18}\text{O}(\text{N}_2\text{O})$ with Eq. (11), which is then compared with the measured $\delta^{18}\text{O}(\text{N}_2\text{O})$ and the difference between measured and calculated $\delta^{18}\text{O}(\text{N}_2\text{O})$ value (D) is determined (Table 4). Since the mean value of 0 was assumed for ε_n in this scenario, the isotope exchange can be associated either with NIR or NOR without any effect on the final $\delta^{18}\text{O}(\text{N}_2\text{O})$, because Eq. (11) is simplified to

$$\frac{\delta - \delta_w}{1 + \delta_w} = (1 - x) \frac{\delta_n - \delta_w}{1 + \delta_w} + x\varepsilon_w. \quad (13)$$

This scenario works quite well for Exp 1 data with the maximal D of 1.4‰. However, for Exp 2 data we obtain significant overestimation of the calculated $\delta^{18}\text{O}(\text{N}_2\text{O})$ values for sandy soils (Exp 2.1 and 2.2) up to 6.1‰ and underestimation for two other soils, reaching up to 12.2‰ for organic soil (Exp 2.5). Why does the model developed based on Exp 1 data not work for Exp 2 data? We expect that the ε_w value should be quite stable for all the samples. It was observed in the study by Casciotti et al. (2007) that $\varepsilon(\text{NO}_2^- / \text{H}_2\text{O})$ values varied in a very narrow range. Also in our study in Fig. 2 we obtained very good correlation with stable slope which suggests that the ε_w value must be very stable and almost identical for all the samples. It can be supposed that ε_n values can be more variable, but due to nearly complete isotope exchange in Exp 1 these potential variations cannot be reflected in $\delta^{18}\text{O}(\text{N}_2\text{O})$ values. Also, the study by Rohe et al. (2014a) indicated possibly wide variations of ε_n from 10 to 30‰.

Therefore, for the next scenarios (Scenario 1, 2 and 3 – Table 4) we assumed a stable ε_w value of 17.5‰, as determined from Exp 1 (Table 3), and ε_n values were calculated individually for each sample with Eq. (11) from the $\delta_0^{18}\text{O}(\text{N}_2\text{O} / \text{H}_2\text{O})$ values. In each scenario ε_n was equally distributed between NIR and NOR according to Eq. (10), so that $\varepsilon_{\text{NIR}} = \varepsilon_{\text{NOR}}$. For our samples we know the value of total isotope exchange (x determined with $\Delta^{17}\text{O}$ method), but we do not know at which enzymatic step(s) this exchange occurred. Since the isotope exchange has very different impact on the final $\delta^{18}\text{O}(\text{N}_2\text{O})$ when associated with NIR or NOR, we can obtain this information by comparing different sce-

narios (Table 4). In Scenario 1 the total isotope exchange is associated with the first reduction step NIR and in Scenario 2, with the final reduction step NOR. In Scenario 3 the total isotope exchange is equally distributed between both steps NIR and NOR according to Eq. (9) so that $x_{\text{NIR}} = x_{\text{NOR}}$.

In this study, we could not determine at which enzymatic step isotope exchange occurs, but only its impact on the implied isotope effects. Namely, in Scenario 1 the exchange effect associated with x_{NIR} precedes the branching effect at NOR (ε_{NOR}) and, conversely, in Scenario 2 the exchange isotope effect associated with x_{NOR} occurs after both branching effects (ε_{NIR} , ε_{NOR}). Hence, in Scenario 1 ε_{NOR} has a more direct impact on the final $\delta^{18}\text{O}(\text{N}_2\text{O})$ whereas in Scenario 2 the last fractionation step is related to ε_w (Eq. 11). Therefore, applying different scenarios results in different values for the calculated ε_n (Table 4).

The narrowest range of variations of the calculated ε_n values was obtained in Scenario 1. For Exp 1 they vary around 0, similarly to the results presented in Table 3, which indicates that this model and the equations applied for $\delta^{18}\text{O}$ method (Eq. 12) are actually the same. For Exp 2 the calculated ε_n values are negative for sandy soils (Exp 2.1 and 2.2) from -9.1 to -6.2 ‰ and positive for other soils with lower values for silt loam from 1.6 to 3.8‰ and higher for organic soil from 3.8 to 18.1‰ (Table 4). Variations of calculated ε_n values are much larger in Scenario 2 with a particularly wide range for Exp 1 from -72.8 to $+38.5$ ‰. For Exp 2, a similar trend as in Scenario 1 is observed, with negative values for sandy soils (down to -20.0 ‰) and highest values for organic soil (up to 37.1‰). The absolute values are generally larger and the variations among them are thereby increased when compared to Scenario 1. The strongly negative ε_n values obtained for Scenario 2 are outside the plausible range based on previous determinations (Casciotti et al., 2007; Rohe et al., 2014a). Moreover, for the last sample of Exp 1 where $x = 1$ this scenario fails in finding the ε_n value for $D = 0$, because for complete isotope exchange by NOR, the associated branching isotope effect has no impact on the final $\delta^{18}\text{O}(\text{N}_2\text{O})$. Hence, Scenario 1 is more plausible because (i) the overall ε_n variations are smaller and (ii) we do not find extremely negative values. Results from Scenario 3 are situated in the middle of Scenario 1 and 2, and show larger variations than Scenario 1, but without the extreme outliers, hence it can be also a plausible model. From comparison of these scenarios we can say that isotope exchange is likely associated with NIR and may also partially take place at NOR (but not NOR alone). This reinforces the previous findings from pure culture studies which suggested that the majority of isotope exchange is associated mainly with nitrite reduction (Garber and Hollocher, 1982; Rohe et al., 2014a). Moreover, each scenario indicates clearly a much lower branching effect for the two sandy soils in Exp 2 when compared to silt loam and organic soil. This is the reason behind the different slope of correlation $\delta_0^{18}\text{O}(\text{N}_2\text{O} / \text{H}_2\text{O})$ vs. x in Fig. 4 for sandy soils. Lower ε_n values mean that N₂O

Table 4. Oxygen fractionation model based on the results obtained ($\delta_0^{18}\text{O}(\text{N}_2\text{O})$) and isotope exchange (x) determined by $\Delta^{17}\text{O}$ method and $\varepsilon_w = 17.5\text{‰}$ determined from Exp 1 data (Table 3). Scenarios with varied ε_n values and x_{NIR} or x_{NOR} (fraction of isotope exchange associated with NIR or NOR) are compared. D is the difference between measured $\delta^{18}\text{O}$ of N₂O and the calculated $\delta^{18}\text{O}$ of N₂O in a particular scenario.

	Scenario 0		Scenario 1		Scenario 2		Scenario 3	
	$x = x_{\text{NIR}}$ or x_{NOR} $\varepsilon_n = 0$ $\varepsilon_w = 17.5\text{‰}$ D	$x_{\text{NIR}} = x$; $x_{\text{NOR}} = 0$ ε_n fitted $\varepsilon_w = 17.5\text{‰}$ ε_n D	$x_{\text{NIR}} = 0$; $x_{\text{NOR}} = x$ ε_n fitted $\varepsilon_w = 17.5\text{‰}$ ε_n D	$x_{\text{NIR}} = x_{\text{NOR}}$ ε_n fitted $\varepsilon_w = 17.5\text{‰}$ ε_n D				
Exp 1.1a	0.2	0.3	0.00	2.3	0.00	1.0	0.00	
	0.6	1.2	0.00	16.0	0.00	5.3	0.00	
Exp 1.1b	0.1	0.2	0.00	2.7	0.00	0.9	0.00	
	-1.2	-2.3	0.00	-22.6	0.00	-8.6	0.00	
Exp 1.1c	0.2	0.4	0.00	4.7	0.00	1.7	0.00	
	0.0	0.1	0.00	0.6	0.00	0.2	0.00	
Exp 1.2a	-0.3	-0.5	0.00	-3.7	0.00	-1.6	0.00	
	-0.8	-1.5	0.00	-18.4	0.00	-6.2	0.00	
	0.3	0.6	0.00	4.5	0.00	1.9	0.00	
	0.2	0.3	0.00	2.7	0.00	1.0	0.00	
Exp 1.2b	-0.4	-0.7	0.00	-4.0	0.00	-1.9	0.00	
	0.1	0.2	0.00	1.7	0.00	0.7	0.00	
	1.4	2.6	0.00	38.5	0.00	12.1	0.00	
	-0.7	-1.3	0.00	-72.8	0.00	-12.5	0.00	
	-0.3	-0.6	0.00	-19.3	0.00	-4.2	0.00	
	0.2	0.4	0.00	0.0	0.22	0.0	0.22	
Exp 2.1	-4.0	-6.2	0.00	-14.7	0.00	-10.0	0.00	
	-5.3	-8.2	0.00	-19.9	0.00	-13.4	0.00	
Exp 2.2	-5.2	-7.6	0.00	-15.0	0.00	-11.0	0.00	
	-6.1	-9.1	0.00	-20.0	0.00	-14.1	0.00	
Exp 2.3	2.5	3.2	0.00	4.9	0.00	4.0	0.00	
	3.0	3.8	0.00	5.7	0.00	4.7	0.00	
Exp 2.4	1.1	1.6	0.00	3.4	0.00	2.4	0.00	
	2.2	2.9	0.00	4.8	0.00	3.8	0.00	
Exp 2.5	2.8	4.2	0.00	8.5	0.00	6.2	0.00	
	12.2	18.1	0.00	37.1	0.00	27.0	0.00	
Exp 2.6	2.2	3.8	0.00	20.9	0.00	10.2	0.00	
	4.2	6.8	0.00	19.1	0.00	12.2	0.00	

is less enriched in ^{18}O in relation to soil nitrate and lower x results in smaller increase in $\delta^{18}\text{O}(\text{N}_2\text{O})$ values, which was observed for sandy soils (Fig. 4).

For each scenario our model indicated rather lower ε_n values than previously assumed (Casciotti et al., 2007; Rohe et al., 2014a). But actually, the isotope effect determined by Casciotti et al. (2007), +25 to +30‰, takes only the intramolecular branching effect into account, because in the bacterial denitrification method the whole nitrate pool is quantitatively consumed, hence the intermolecular isotope effect cannot manifest. Therefore, the values found by Casciotti et al. (2007) represent the maximal possible branching effect. In the experiment presented by Rohe et al. (2014a) only very little added substrate was reduced, hence we should also observe the intermolecular isotope effects. Indeed, the

model applied by Rohe et al. (2014a) indicated lower magnitudes for net branching, down to +10‰ for ε_{NIR} and 0‰ for ε_{NAR} . This may suggest that the net branching effect decreases with smaller reaction rates because of intermolecular isotope effects. But are negative net branching effects actually possible? The answer is yes, provided that the intermolecular effect exceeds the intramolecular effect, i.e. the former must be more negative than -30‰. An idea about the magnitude of the intermolecular effect can be obtained from the change in isotopic signature of the remaining nitrate, since this reflects the enrichment in residual nitrate- ^{18}O due to intermolecular effects. In pure culture studies this effect ranges from -23 to -5‰ (Granger et al., 2008), but in soil incubations values as low as -37‰ have been observed (Exp. 1F in Lewicka-Szczebak et al., 2014). Hence, slightly

negative net ϵ_n values are theoretically possible, but up to a few ‰ for each enzymatic step, which gives the minimal overall ϵ_n of about -10 ‰. Therefore, the results of Scenario 2 must be rejected, whereas the values found in Scenario 1 are most plausible.

3.6 Significance for quantification and differentiation of soil denitrification

From the presented results it is most surprising and incomprehensible why the same soils show various extents of isotope exchange with soil water, and especially, why this exchange was high and stable under static anoxic conditions and significantly lower in flow-through incubations. Most probably, in the static inhibited experiments denitrification is the only N₂O producing process and in the flow-through uninhibited incubations other N₂O producing processes may significantly contribute to N₂O production. These incubations were performed initially under oxic conditions, which were switched to anoxic conditions after 3 days. However, all the results presented here originate from this anoxic phase, since the N₂O production during oxic phase was too low for $\Delta^{17}\text{O}$ analyses. Hence, the potentially contributing processes might be fungal denitrification, co-denitrification, nitrifier denitrification or dissimilatory nitrate reduction to ammonium (DNRA). ¹⁵N site preference ($\delta^{15}\text{N}^{\text{SP}}$) may be used as a tracer to distinguish some of these processes. It is known that fungal denitrification and nitrification are characterized by significantly higher $\delta^{15}\text{N}^{\text{SP}}$ values (33 to 37 ‰, Rohe et al., 2014a; Sutka et al., 2006, 2008) when compared to bacterial denitrification and nitrifier denitrification (-11 to 0 ‰, Sutka et al., 2006; Toyoda et al., 2005). To check the hypothesis of mixing of N₂O from various sources we plotted $\delta_0^{18}\text{O}(\text{N}_2\text{O}/\text{H}_2\text{O})$ values against $\delta_0^{15}\text{N}^{\text{SP}}$ values of produced N₂O (Fig. 5).

It can be clearly noticed that the results from the inhibited experiment (Exp 1, red symbols) fit perfectly into the field of bacterial denitrification. Similarly, the results of sandy soils from Exp 2 show a slightly wider range, but still are typical for bacterial denitrification. In contrast, silt loam soil (Exp 2.3, 2.4) and organic soil (Exp 2.5, 2.6) both show increased $\delta_0^{18}\text{O}(\text{N}_2\text{O}/\text{H}_2\text{O})$ and $\delta_0^{15}\text{N}^{\text{SP}}$ values which are very well correlated. This could indicate that in Exp 2 another process characterized by high $\delta^{15}\text{N}^{\text{SP}}$ and $\delta^{18}\text{O}$ values has significant contribution to total N₂O production by these two soils. This could be nitrification, which is not very plausible due to the anoxic conditions, or fungal denitrification. But it remains unclear why this was not observed in the inhibited static incubation for the same soil (silt loam). C₂H₂ inhibition does not affect fungal denitrification (Maeda et al., 2015) in that NO₃⁻ and NO₂⁻ availability is not restricted by inhibited nitrification. However, in the flow-through incubations, the first oxic phase might have activated other microorganisms, possibly preferentially fungi. This could explain why their contribution is observed in Exp 2 but not in Exp 1. Such

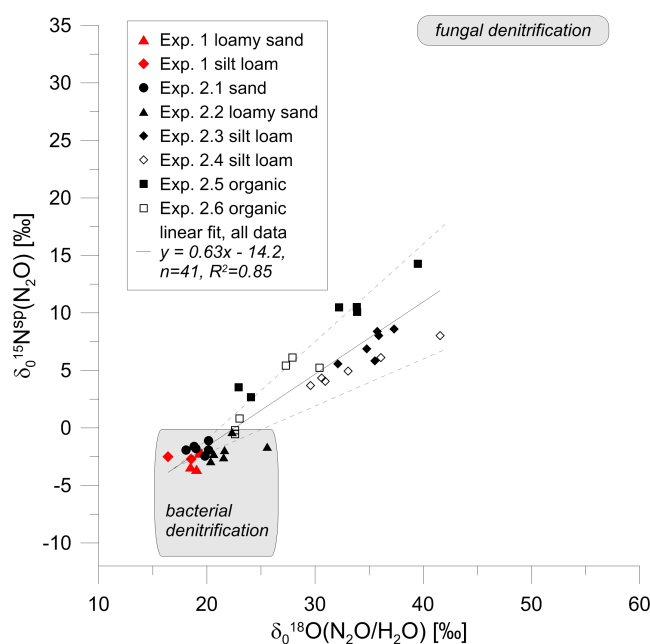


Figure 5. Relation between $\delta_0^{15}\text{N}^{\text{SP}}$ of produced N₂O and relative ratio difference between produced N₂O and soil water ($\delta_0^{18}\text{O}(\text{N}_2\text{O}/\text{H}_2\text{O})$). Red symbols: Exp 1; black symbols: Exp 2; open symbols: incubations with lower WFPS (70 %); filled symbols: incubations with higher WFPS (80 %). Note that the same symbol shapes always represent the same soil. Grey dashed lines represent the possible range of linear fit when extreme values of isotope effects for N₂O reduction are assumed in correction calculations (Eq. 5). Range of values for fungal denitrification from Rohe et al. (2014a).

an activation of denitrification by oxygen supply has been documented for one fungus species (Zhou et al., 2001).

We checked whether the correlation presented in Fig. 5 could have resulted from calculation artifacts, since all of the higher $\delta_0^{18}\text{O}(\text{N}_2\text{O}/\text{H}_2\text{O})$ and $\delta_0^{15}\text{N}^{\text{SP}}$ values were corrected for N₂O reduction (according to the method described in Sect. 2.5). This correction method does not provide very precise results, since the isotope effects associated with N₂O reduction are not entirely stable and predictable (Lewicka-Szczebak et al., 2014, 2015). Therefore, we checked whether this correlation may be only a calculation artifact and recalculated the values assuming larger range of isotopic fractionations (± 5 ‰, resulting in $\epsilon^{15}\text{N}^{\text{SP}}(\text{N}_2/\text{N}_2\text{O})$ from -10 to 0 ‰ and $\epsilon^{18}\text{O}(\text{N}_2/\text{N}_2\text{O})$ from -20 to -6 ‰). Results show that the correlation may slightly change in slope (from 0.41 to 0.85), intercept (from -10.4 to -18.0) and significance (R^2 from 0.64 to 0.91). But it always keeps the same trend, i.e. for Exps 2.3–2.6 we obtain in any case a correlated increase of $\delta_0^{15}\text{N}^{\text{SP}}$ and $\delta_0^{18}\text{O}(\text{N}_2\text{O}/\text{H}_2\text{O})$ (see grey dashed lines in Fig. 5), proving that the indication for further contributing processes cannot be an artifact of the correction approach. For these experiments (2.3–2.6) in our model calculations (Table 4) higher ϵ_n values were always found when

compared to Exp 1 and 2.1–2.2. For pure culture studies of fungal denitrification the ϵ_n values determined by a similar modelling approach were also higher, up to 30 ‰ (Rohe et al., 2014a). This would support the hypothesis on fungal denitrification contribution.

3.7 Source of $\Delta^{17}\text{O}$ in atmospheric N₂O

In Exp 1 the $\Delta^{17}\text{O}(\text{N}_2\text{O})$ values obtained from all measured N₂O samples were very low. Moreover, we also included the treatment with chemical nitrate as fertilizer, characterized by slightly negative $\Delta^{17}\text{O}$ excess (of ca. -1.5 ‰), and the produced N₂O did not show any positive $\Delta^{17}\text{O}$ excess (results not shown). The produced N₂O is always characterized by smaller ^{17}O excess ($\Delta^{17}\text{O}$ values closer to 0) than in the source nitrate (Table 1). These results indicate that denitrification produces N₂O of randomly distributed oxygen, due to a mostly very high extent of isotope exchange with soil water and the consequent loss of ^{17}O excess of nitrate. However, in Exp 2 numerous samples showed lower extent of isotope exchange, down to 50 %, and the ^{17}O excess of nitrate is partially transferred to N₂O, resulting in $\Delta^{17}\text{O}(\text{N}_2\text{O})$ up to 5 ‰. This indicates that denitrification may be the source of atmospheric N₂O with ^{17}O excess, as previously supposed (Kaiser et al., 2004; Michalski et al., 2003), but the magnitude of this excess is largely reduced by the exchange of oxygen isotopes with randomly distributed soil water.

4 Conclusions

It can be supposed that bacterial denitrification in soils is characterized by quite stable $\delta_0^{18}\text{O}(\text{N}_2\text{O}/\text{H}_2\text{O})$ of 17.5 ± 1.2 ‰ due to the nearly complete O isotope exchange and constant isotope effect associated with this exchange. Hence, when N₂O producing processes other than heterotrophic processes are negligible, $\delta_0^{18}\text{O}(\text{N}_2\text{O})$ can be well predicted. Conversely, $\delta_0^{18}\text{O}(\text{N}_2\text{O}/\text{H}_2\text{O})$ values larger than 19 ‰ are probably indicative of the contribution of other processes. However, more work on oxygen isotope effects during N₂O production by various microorganisms is needed to obtain robust estimate of their contribution. It is necessary to conduct experiments to determine the possible range of $\delta_0^{18}\text{O}(\text{N}_2\text{O}/\text{H}_2\text{O})$ for different N₂O-forming processes. From the studies available until now, we can make a first estimate for $\delta_0^{18}\text{O}(\text{N}_2\text{O}/\text{H}_2\text{O})$ characteristic of fungal denitrification of (48.2 ± 3.7) ‰ (when disregarding two most extreme values; for all results (47.4 ± 10.3) ‰) (Rohe et al., 2014a). This value is very different from the $\delta_0^{18}\text{O}(\text{N}_2\text{O}/\text{H}_2\text{O})$ of bacterial denitrification determined here, i.e. (17.5 ± 1.2) ‰. This opens up a new perspective of applying $\delta_0^{18}\text{O}(\text{N}_2\text{O}/\text{H}_2\text{O})$ for differentiation between fungal and bacterial denitrification.

The Supplement related to this article is available online at doi:10.5194/bg-13-1129-2016-supplement.

Acknowledgements. This study was supported by the German Research Foundation (DFG We/1904-4). Many thanks are due to Anette Giesemann and Martina Heuer for help in N₂O isotopic analyses, Lars Szvec for $\Delta^{17}\text{O}$ analyses, Kerstin Gilke for help in chromatographic analyses, Caroline Buchen for supplying soil for laboratory incubations and Maciej Lewicki for supplying the isotopically depleted water from the Tatra Mountains, Poland.

Edited by: Y. Kuzyakov

References

- Böhlke, J. K., Mroczkowski, S. J., and Coplen, T. B.: Oxygen isotopes in nitrate: new reference materials for ^{18}O : ^{17}O : ^{16}O measurements and observations on nitrate-water equilibration, *Rapid Commun. Mass Sp.*, 17, 1835–1846, 2003.
- Butterbach-Bahl, K., Willibald, G., and Papen, H.: Soil core method for direct simultaneous determination of N₂ and N₂O emissions from forest soils, *Plant Soil*, 240, 105–116, 2002.
- Casciotti, K. L., Sigman, D. M., Hastings, M. G., Böhlke, J. K., and Hilke, A.: Measurement of the oxygen isotopic composition of nitrate in seawater and freshwater using the denitrifier method, *Anal. Chem.*, 74, 4905–4912, 2002.
- Casciotti, K. L., Böhlke, J. K., McIlvin, M. R., Mroczkowski, S. J., and Hannon, J. E.: Oxygen isotopes in nitrite: Analysis, calibration, and equilibration, *Anal. Chem.*, 79, 2427–2436, 2007.
- Dyckmans, J., Lewicka-Szczebak, D., Szvec, L., Langel, R., and Well, R.: Comparison of methods to determine triple oxygen isotope composition of N₂O, *Rapid Commun. Mass Sp.*, 29, 1991–1996, 2015.
- Eickenscheidt, T., Heinichen, J., Augustin, J., Freibauer, A., and Drösler, M.: Nitrogen mineralization and gaseous nitrogen losses from waterlogged and drained organic soils in a black alder (*Alnus glutinosa* (L.) Gaertn.) forest, *Biogeosciences*, 11, 2961–2976, doi:10.5194/bg-11-2961-2014, 2014.
- Garber, E. A. E. and Hollocher, T. C.: ^{15}N , ^{18}O Tracer Studies on the Activation of Nitrite by Denitrifying Bacteria – Nitrite Water-Oxygen Exchange and Nitrosation Reactions as Indicators of Electrophilic Catalysis, *J. Biol. Chem.*, 257, 8091–8097, 1982.
- Granger, J., Sigman, D. M., Lehmann, M. F., and Tortell, P. D.: Nitrogen and oxygen isotope fractionation during dissimilatory nitrate reduction by denitrifying bacteria, *Limnol. Oceanogr.*, 53, 2533–2545, 2008.
- IPCC: The Physical Science Basis, Contribution of Working Group I to the Fifth Assessment Report of the Intergovernmental Panel on Climate Change, Intergovernmental Panel on Climate Change, Cambridge, United Kingdom and New York, NY, USA, 996 pp., 1535 pp., 2013.
- Kaiser, J. and Röckmann, T.: Correction of mass-spectrometric isotope ratio measurements for isobaric isotopologues of O₂, CO, CO₂, N₂O and SO₂, *Rapid Commun. Mass Spectr.*, 22, 3997–4008, 2008.

- Kaiser, J., Rockmann, T., and Brenninkmeijer, C. A. M.: Contribution of mass-dependent fractionation to the oxygen isotope anomaly of atmospheric nitrous oxide, *J. Geophys. Res.-Atmos.*, 109, 1–10, 2004.
- Kaiser, J., Hastings, M. G., Houlton, B. Z., Rockmann, T., and Sigman, D. M.: Triple oxygen isotope analysis of nitrate using the denitrifier method and thermal decomposition of N₂O, *Anal. Chem.*, 79, 599–607, 2007.
- Königer, P., Marshall, J. D., Link, T., and Mulch, A.: An inexpensive, fast, and reliable method for vacuum extraction of soil and plant water for stable isotope analyses by mass spectrometry, *Rapid Commun. Mass Sp.*, 25, 3041–3048, 2011.
- Kool, D. M., Wrage, N., Oenema, O., Dolfing, J., and Van Groenigen, J. W.: Oxygen exchange between (de) nitrification intermediates and H₂O and its implications for source determination of NO₃⁻ and N₂O: a review, *Rapid Commun. Mass Sp.*, 21, 3569–3578, 2007.
- Kool, D. M., Wrage, N., Oenema, O., Harris, D., and Van Groenigen, J. W.: The ¹⁸O signature of biogenic nitrous oxide is determined by O exchange with water, *Rapid Commun. Mass Sp.*, 23, 104–108, 2009.
- Lewicka-Szczebak, D., Well, R., Giesemann, A., Rohe, L., and Wolf, U.: An enhanced technique for automated determination of ¹⁵N signatures of N₂, (N₂+N₂O) and N₂O in gas samples, *Rapid Commun. Mass Sp.*, 27, 1548–1558, 2013.
- Lewicka-Szczebak, D., Well, R., Koster, J. R., Fuss, R., Senbayram, M., Dittert, K., and Flessa, H.: Experimental determinations of isotopic fractionation factors associated with N₂O production and reduction during denitrification in soils, *Geochim. Cosmochim. Ac.*, 134, 55–73, 2014.
- Lewicka-Szczebak, D., Well, R., Bol, R., Gregory, A., Matthews, P., Misselbrook, T., Whalley, R., and Cardenas, L.: Isotope fractionation factors controlling isotopic signatures of soil-emitted N₂O produced by denitrification processes of various rates, *Rapid Commun. Mass Sp.*, 29, 269–282, 2015.
- Maeda, K., Spor, A., Edel-Hermann, V., Heraud, C., Breuil, M. C., Bizouard, F., Toyoda, S., Yoshida, N., Steinberg, C., and Philippot, L.: N₂O production, a widespread trait in fungi, *Sci. Rep.-Uk.*, 5, 1–7, 2015.
- Mariotti, A., Germon, J. C., Hubert, P., Kaiser, P., Letolle, R., Tardieux, A., and Tardieux, P.: Experimental determination of nitrogen kinetic isotope fractionation – some principles – illustration for the denitrification and nitrification processes, *Plant Soil*, 62, 413–430, 1981.
- Michalski, G., Scott, Z., Kabling, M., and Thiemens, M. H.: First measurements and modeling of Delta ¹⁷O in atmospheric nitrate, *Geophys. Res. Lett.*, 30, 14-1–14-4, 2003.
- Mohn, J., Wolf, B., Toyoda, S., Lin, C. T., Liang, M. C., Bruggemann, N., Wissel, H., Steiker, A. E., Dyckmans, J., Szewc, L., Ostrom, N. E., Casciotti, K. L., Forbes, M., Giesemann, A., Well, R., Doucet, R. R., Yarnes, C. T., Ridley, A. R., Kaiser, J., and Yoshida, N.: Interlaboratory assessment of nitrous oxide isotopomer analysis by isotope ratio mass spectrometry and laser spectroscopy: current status and perspectives, *Rapid Commun. Mass Sp.*, 28, 1995–2007, 2014.
- Opdyke, M. R., Ostrom, N. E., and Ostrom, P. H.: Evidence for the predominance of denitrification as a source of N₂O in temperate agricultural soils based on isotopologue measurements, *Global Biogeochem. Cy.*, 23, GB4018, doi:10.1029/2009gb003523, 2009.
- Ostrom, N. E., Pitt, A., Sutka, R., Ostrom, P. H., Grandy, A. S., Huizinga, K. M., and Robertson, G. P.: Isotopologue effects during N₂O reduction in soils and in pure cultures of denitrifiers, *J. Geophys. Res.-Biogeo.*, 112, G02005, doi:10.1029/2006jg000287, 2007.
- Park, S., Perez, T., Boering, K. A., Trumbore, S. E., Gil, J., Marquina, S., and Tyler, S. C.: Can N₂O stable isotopes and isotopomers be useful tools to characterize sources and microbial pathways of N₂O production and consumption in tropical soils?, *Global Biogeochem. Cy.*, 25, GB1001, doi:10.1029/2009gb003615, 2011.
- Perez, T., Garcia-Montiel, D., Trumbore, S., Tyler, S., De Camargo, P., Moreira, M., Piccolo, M., and Cerri, C.: Nitrous oxide nitrification and denitrification ¹⁵N enrichment factors from Amazon forest soils, *Ecol. Appl.*, 16, 2153–2167, 2006.
- Ravishankara, A. R., Daniel, J. S., and Portmann, R. W.: Nitrous Oxide (N₂O): The Dominant Ozone-Depleting Substance Emitted in the 21st Century, *Science*, 326, 123–125, 2009.
- Röckmann, T., Kaiser, J., Brenninkmeijer, C. A. M., and Brand, W. A.: Gas chromatography/isotope-ratio mass spectrometry method for high-precision position-dependent ¹⁵N and ¹⁸O measurements of atmospheric nitrous oxide, *Rapid Commun. Mass Sp.*, 17, 1897–1908, 2003.
- Rohe, L., Anderson, T.-H., Braker, G., Flessa, H., Giesemann, A., Lewicka-Szczebak, D., Wrage-Mönnig, N., and Well, R.: Dual isotope and isotopomer signatures of nitrous oxide from fungal denitrification – a pure culture study, *Rapid Commun. Mass Sp.*, 28, 1893–1903, 2014a.
- Rohe, L., Anderson, T. H., Braker, G., Flessa, H., Giesemann, A., Wrage-Mönnig, N., and Well, R.: Fungal oxygen exchange between denitrification intermediates and water, *Rapid Commun. Mass Sp.*, 28, 377–384, 2014b.
- Schmidt, H. L., Werner, R. A., Yoshida, N., and Well, R.: Is the isotopic composition of nitrous oxide an indicator for its origin from nitrification or denitrification? A theoretical approach from referred data and microbiological and enzyme kinetic aspects, *Rapid Commun. Mass Sp.*, 18, 2036–2040, 2004.
- Scholefield, D., Hawkins, J. M. B., and Jackson, S. M.: Development of a helium atmosphere soil incubation technique for direct measurement of nitrous oxide and dinitrogen fluxes during denitrification, *Soil Biol. Biochem.*, 29, 1345–1352, 1997.
- Snider, D., Venkiteswaran, J. J., Schiff, S. L., and Spoelstra, J.: A new mechanistic model of δ¹⁸O-N₂O formation by denitrification, *Geochim. Cosmochim. Ac.*, 112, 102–115, 2013.
- Snider, D. M., Schiff, S. L., and Spoelstra, J.: ¹⁵N/¹⁴N and ¹⁸O/¹⁶O stable isotope ratios of nitrous oxide produced during denitrification in temperate forest soils, *Geochim. Cosmochim. Ac.*, 73, 877–888, 2009.
- Snider, D. M., Venkiteswaran, J. J., Schiff, S. L., and Spoelstra, J.: Deciphering the oxygen isotope composition of nitrous oxide produced by nitrification, *Glob. Change Biol.*, 18, 356–370, 2012.
- Stein, L. Y. and Yung, Y. L.: Production, isotopic composition, and atmospheric fate of biologically produced nitrous oxide, *Annu. Rev. Earth. Pl. Sc.*, 31, 329–356, 2003.
- Sutka, R. L., Ostrom, N. E., Ostrom, P. H., Gandhi, H., and Breznak, J. A.: Nitrogen isotopomer site preference of N₂O produced

- by *Nitrosomonas europaea* and *Methylococcus capsulatus* Bath, *Rapid Commun. Mass Sp.*, 17, 738–745, 2003.
- Sutka, R. L., Ostrom, N. E., Ostrom, P. H., Breznak, J. A., Gandhi, H., Pitt, A. J., and Li, F.: Distinguishing nitrous oxide production from nitrification and denitrification on the basis of isotopomer abundances, *Appl. Environ. Microb.*, 72, 638–644, 2006.
- Sutka, R. L., Adams, G. C., Ostrom, N. E., and Ostrom, P. H.: Isotopologue fractionation during N₂O production by fungal denitrification, *Rapid Commun. Mass Sp.*, 22, 3989–3996, 2008.
- Toyoda, S. and Yoshida, N.: Determination of nitrogen isotopomers of nitrous oxide on a modified isotope ratio mass spectrometer, *Anal. Chem.*, 71, 4711–4718, 1999.
- Toyoda, S., Mutoke, H., Yamagishi, H., Yoshida, N., and Tanji, Y.: Fractionation of N₂O isotopomers during production by denitrifier, *Soil Biol. Biochem.*, 37, 1535–1545, 2005.
- Toyoda, S., Yano, M., Nishimura, S., Akiyama, H., Hayakawa, A., Koba, K., Sudo, S., Yagi, K., Makabe, A., Tobari, Y., Ogawa, N. O., Ohkouchi, N., Yamada, K., and Yoshida, N.: Characterization and production and consumption processes of N₂O emitted from temperate agricultural soils determined via isotopomer ratio analysis, *Global Biogeochem. Cy.*, 25, GB2008, doi:10.1029/2009gb003769, 2011.
- Well, R. and Flessa, H.: Isotopologue enrichment factors of N₂O reduction in soils, *Rapid Commun. Mass Sp.*, 23, 2996–3002, 2009.
- Well, R., Flessa, H., Xing, L., Ju, X. T., and Romheld, V.: Isotopologue ratios of N₂O emitted from microcosms with NH₄⁺ fertilized arable soils under conditions favoring nitrification, *Soil Biol. Biochem.*, 40, 2416–2426, 2008.
- Westley, M. B., Popp, B. N., and Rust, T. M.: The calibration of the intramolecular nitrogen isotope distribution in nitrous oxide measured by isotope ratio mass spectrometry, *Rapid Commun. Mass Sp.*, 21, 391–405, 2007.
- Zhou, Z. M., Takaya, N., Sakairi, M. A. C., and Shoun, H.: Oxygen requirement for denitrification by the fungus *Fusarium oxysporum*, *Arch. Microbiol.*, 175, 19–25, 2001.